[7] Engel, W. N., Cochran, R. L., and Delao, M. M., "Use of Axial Flow Pumps for Marine Propulsion," Paper 442A, January 8–12, 1962, Society of Automotive Engineers, Detroit, Mich.

[8] Gongwer, C. A., "The Influence of Duct Losses on Jet Propulsion Devices," *Jet Propulsion*, Vol. 24, Nov.-Dec. 1954, pp. 385–386.

[9] Bailey, W. S. et al., "Gas-Particle Flow in an Axisymmetric Nozzle," *ARS Journal*, Vol. 31, June 1961, pp. 793–798.

[10] Elliott, D. G., "Analysis of the Acceleration of Lithium in a Two-Phase Nozzle," *Proceedings of 1963 High-Temperature Liquid Metal Heat Transfer Technology Meeting*, Oak Ridge, Tenn., Dec. 1964.

[11] Lane, W. R. and Green, H. L., "The Mechanics of Drops and Bubbles," *Surveys in Mechanics*, Cambridge University, London, 1956, pp. 162–215.

[12] Scott, D. S., "Properties of Concurrent Gas-Liquid Flow," *Advances in Chemical Engineering*, Vol. 4, Academic Press, New York, 1963, pp. 200–278.

[13] Martinelli, R. D. and Nelson, D. B., "Prediction of Pressure Drop During Forced Circulation Boiling of Water," *Transactions of the American Society of Mechanical Engineers*, Vol. 70, A 1948, pp. 695–702.

[14] Vance, W. H. and Moulton, R. W., "A Study of Slip Rat for the Flow of Steam-Water Mixtures at High Void Fraction *American Institute of Chemical Engineers Journal*, Vol. 11, N 1965, pp. 1114–1124.

[15] Arcand, L., "Waterjet Propulsion for Small Craft," Pa F, Southwest Section Meeting, May 26–28, 1966, Society Naval Architects and Marine Engineers, Miami, Fla.

[16] Tulen, M. P., "Supercavitating Propellers—History, Oper ing Characteristics, and Mechanism of Operation," *Proceedi of Fourth ONR Symposium on Naval Hydrodynamics*, 19 Washington, D. C.

[17] Gill, J. D., "The Hydrofoil Commuter," *Boat Construct and Maintenance*, Feb. 1965.

[18] "Fact Sheet, FT3C-9 Marine Gas Turbine," May 17, 19 Pratt & Whitney Aircraft, East Hartford, Conn.

[19] "A Parametric Study of Hydrofoil Ships," U.S. Na Bureau of Ships Rept. D2-20671-3, Dec. 1963, The Boeing C Seattle, Wash.

JANUARY 1968 J. HYDRONAUTICS VOL. 2, NO

Selection and Utilization of Batteries for Deep Submergence Vehicles

N. KUSKA* AND J. A. CRONANDER†
North American Rockwell Corporation, Long Beach, Calif.

A brief review of battery characteristics is presented. The mission parameters of a deep submergence vehicle that affect battery cell selection are mentioned, as well as a few of the pitfalls and problem areas which can be encountered. The conception and design of a battery container system is discussed, including electrolyte reservoirs, pressure compensators and gas vent valves. The results of a battery system test program are covered including capacity, charging, gassing, and significant findings.

Introduction

As dive depths of submersible vehicles increased, ways to reduce weight or increase buoyancy became paramount. This led to power system storage batteries external to the pressure hull. In this location, they could be operated at ambient sea pressure, wherein a savings in volume and weight could be realized. Problems of temperature control and ventilation became ones of pressure compensation, insulation, and material compatibility, with a few added ones of maintenance, control, and reliability.

Characteristics of Candidate Cells

Table 1 presents some characteristics of candidate cell types. Lead-acid cells have been used on most deep submergence vehicles where the batteries are located external to the pressure hull. Except when low-energy density rules out the lead-acid battery, it will probably see extensive use for a long time to come. It is a proven, inexpensive, rugged, reliable, and relatively easy-to-service source of power. It also has a high cell voltage, relatively long cycle life, and trou free service life. There are no off-the-shelf units desig specifically for use external to the pressure hull. All insta tions have been adaptations of automobile, truck, golf cart, industrial cells. This has resulted in larger, heavier, and, some cases, shorter lived installations than could be obtai from cells especially designed for the ocean environment.

Silver-zinc cells are currently being developed for d submersible use in the ocean environment. This cell typ characterized by its high energy density, tolerance to h rates of discharge, and long dry-storage life. Its dis vantages are high cost, short cycle life for deep discha cycles, short wet-storage life, and difficulty in determin state of charge.

The silver-cadmium cell combines the high energy dens of the silver anode with the long life of the cadmium catho As was shown in Table 1, the energy density is somewhat l than that of silver-zinc, but the increased cycle life may ov come this for some applications. Cost per cell is close to t of silver-zinc, but more cells are required because the nomi cell voltage is lower. The silver-cadmium battery can charged fast and has a long dry-storage life.

Mission

Factors in a deep submersible mission which can aff battery selection are dive depth, energy requirements, sponse time, standby requirements, and permissible ma

Presented as Paper 67-368 at the AIAA/SNAME Advance Marine Vehicles Meeting, Norfolk, Va., May 22–24, 1967; submitted May 22, 1967; revision received September 27, 1967.

* Chief, Subsystems and Components, Ocean Systems Operations.

† Member, Technical Staff, Ocean Systems Operations.

tenance requirements. Required dive depth, if much over 6000 ft, and nominal energy requirements will place a premium on available space and allowable weight. This generally will require a high specific energy, high-cost power system to prevent the round-robin increase of buoyancy requirements, drag, and additional power requirements which could accompany the use of a less compact power-storage system.

Energy requirements will determine battery size and weight once the cell type and depth of discharge have been selected. This selection can have a direct influence on hull size and configuration. Peak power drains could influence cell selection or affect choice of cell construction after a specific couple has been selected. Some cell types are less degraded by high discharge rates, whereas others are more responsive to low rates.

Mission response time or turn-around time can influence battery charge time, which, in turn, could affect average power available, mandatory maintenance period, and cell life. Limitations on charge time tend to move available capacity per cycle toward the discharge side of the voltage time curve. This reduces voltage control and increases the likelihood of inadvertent cell reversal or premature dive termination to prevent it. Reduced charge time may require charging at a high current rate, which, if too high, can generate heat and produce gassing. Excessive heat and gassing will reduce cell life and can cause cell failure if allowed to continue. Excessive gassing will increase periodic maintenance requirements because of water loss by electrolysis.

Standby requirements will affect charge condition or the procedure necessary to maintain charge. It can also affect per cycle cost if utilization rate is low. Limitations on periodic maintenance can place constraints on cell selection if power requirements are not overriding and would certainly affect system design to some degree.

Battery Cycle Life

Probably the most important factor affecting over-all power system cost is battery cycle life which, unfortunately, is one of the most elusive factors in the selection and performance of electrochemical couples. The lack of data or, more specificially, the lack of correlating data, lead to doubt or low confidence in regard to the anticipated life of a given battery installation.

Several factors do affect battery life and should be optimized within the limits of other constraints to obtain as high a cell life as possible. Cycle life sensitivity to depth of discharge is probably the most important, primarily for the silver-zinc combination with silver-cadmium and lead-acid following in decreasing order of vulnerability.

Percent recharge is another factor that should be neither too low, which would allow the battery to discharge deeper in each cycle, nor too high, which could damage the cell by excess temperature and excessive water or active material loss. It has been stated that recharging a cell in each cycle to the value of the previous discharge will lead shortly to cell exhaustion. This means that cell inefficiencies are applicable, to some extent, to cycling at all states of charge and not just to overrate charge and overcapacity charge.

By following appropriate guidelines of evaluation and selection, one would expect to obtain a near-optimum battery power system within the framework of the design requirements. To realize this goal, the finished system should be operated within the established parameters. If this is not the case, projected performance and cost should be re-evaluated in light of the changes, or the system should be modified, if possible, to rectify the discrepancy. In the event that the system falls short of expectations while being operated within established criteria, the system suffers untimely derating. One instance of capacity derating which occurred on a contemporary submersible apparently was due to the cell type selected. Other reasons for derating after the fact could be 1) reduction of usable capacity to obtain more reserve capacity, 2) reduction of usable capacity (depth of discharge) to extend cycle life, 3) reduction of usable capacity due to the replacement of silver electrode cells with less expensive types as an economy move, and 4) reduction of usable capacity when compensating oil is masking plate area because of lowering electrolyte level due to lack of cell maintenance.

Power System Optimization

An optimum battery power system would be one that offered the highest energy density, longest life, minimum care, and the lowest cost consistent with mission and configuration constraints. Unfortunately, not all these attributes are enjoyed by any one electrochemical couple. The primary difference is high energy density-high cost, on the one hand, and low energy density-low cost, on the other. This difference is accentuated more so when cycle life and wet shelf life are included. The immediate effects of this dilemma are high costs if energy requirements are mandatory, and lower energy if cost factors are overriding. It is possible to reduce the cost of a silver electrode system for reducing discharge depth to gain cycle life. This will increase the size of the battery in terms of rated capacity and increase the cost per battery, but may result in a net cost savings over the life of the submarine. Now an added constraint, wet life, primarily for silver-zinc cells comes into the picture, and the desired cycle life may not be obtainable. This factor also precludes a smooth tradeoff transition between silver-zinc and lead-acid when cost as well as discharge depth and cycle life are involved. It is possible to evaluate these factors for a specific couple and attempt a near optimum configuration on a cost basis if some flexibility can be obtained on system size and weight.

Figure 1 is a plot of power system cost vs percent of discharge for a silver-zinc system. It depicts curves of constant energy supply. A minimum-cost, silver-zinc system would occur where a utilization rate curve intersects the applicable replacement rate curve since continued reduction in discharge depth would result in increased costs. It is interesting to note that high utilization rates dictate shallow discharge for economy, and low utilization rates dictate deep discharge.

Table 1 Nominal battery characteristics

Types	Energy density[a]		No. of cells for 12-v battery	Voltage per cell		Estimated life[b]	
	W-hr/lb	W-hr-/in^3		open circ.	av. voltage	cycles	yr
Lead-acid (automotive)	15	1.3	6	2.1	1.9	50–300	3
Lead-acid (industrial)	11	1.1	6	2.1	1.9	1600	5–10
Silver-zinc	50	3.0	8	1.86 1.58	1.55	100–200	1
Silver-cadmium	30	2.5	11	1.40 1.12	1.06	500	2–3

[a] Can vary considerably as a function of design.
[b] Can vary considerably as a function of design, usage, and maintenance.

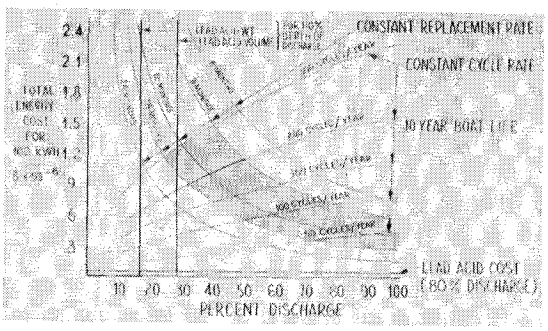

Fig. 1 Power source cost. Constant energy ~ silver-zinc.

Shown also are the limits where system volume or weight, with decreased depth of discharge, arrive at those of lead-acid.

The Fig. 1 plot was obtained by generating arbitrary replacement rate cost curves, using current unit price information. The constant cycle rate curves were obtained from life-cycle test data from Refs. 1 and 2 and manufacturer's test data. The shaded area depicts the area wherein most systems would lie. The trend of the constant cycle rate curves can be a matter for conjecture and is certainly sensitive to additional breakthroughs in cell cycle life of which we are not aware. Regardless of the exact trend, the utility of the plot is not necessarily affected.

Design of Battery Container System

After the selection of battery cell type, size, and number, the task becomes one of providing an appropriate insulation, compensation, and gas removal (ICR) system for the battery to function properly in the ambient pressure and temperature cycling it will experience throughout its usable life. The basic functions of an ICR system are to provide required electrical insulation, to compensate the battery to ambient sea pressure, to prevent leakage, to provide electrolyte level control, and to provide efficient removal of generated gases.

Insulation can be accomplished either by placing the cells in an oil-filled box or by potting the cell tops to provide the required insulation. The oil should be one that is relatively unaffected by and nonmiscible in seawater, weak sulfuric acid solutions for lead-acid cells, or potassium hydroxide solutions for the alkaline cells. It should also be unaffected by battery gases and possess good dielectric properties. The cell top terminal potting should possess good dielectric properties and not absorb water at high pressure. It should provide good adhesion properties to cell top and electrical insulation materials, and it should stand up to the mechanical abuse it will experience in service.

The pressure compensator may consist of an elastic member, which contains a sufficient volume of oil to supply the battery throughout the extremes of pressure, temperature, and entrained gas volumes to which the battery will be exposed. For the purpose of obtaining a positive internal pressure to prevent ingesting seawater, it is possible to superimpose on the ambient sea pressure, the pressure generated by the spring rate of the elastic member or of an auxiliary spring. It is also possible, by proper location of the compensator, that the differential density head between seawater and compensating oil will generate the internal pressure. The pressure compensator fluid should be associated with reservoirs that are attached to each cell top in which the interface between electrolyte and oil occurs. The reservoir should be sized so as to maintain the electrolyte oil interface within prescribed limits at all times. The outlet of the reservoir should contain a simple baffle system to enhance the removal of acid droplets from departing gas bubbles.

The system should contain pressure-relief provisions so that generated gases may be vented overboard. This valve should be leak-proof to prevent expulsion of the compensating oil over a period of time and jam-free to prevent cell or system damage due to gas-generated internal pressure.

Cell Top Reservoir

Assuming that oil is not to enter the cell top where it could contact plates, the reservoir volume below the acid removal baffles should include, as a minimum, the following incremental volumes:

1) Volume change due to compressibility

$$\Delta V_c = V_0 \Delta P / B_{\text{ave}}$$

where

V_0 = electrolyte volume = $V_{\text{cell}} + V_{\text{fill}}$
B_{ave} = average electrolyte bulk modulus
ΔP = depth pressure

2) Volume change due to temperature

$$\Delta V_t = \alpha_t V_0 \Delta T$$

where α_t = volumetric temperature expansion coefficient of electrolyte and ΔT = temperature change.

3) Mechanically trapped gas volume $\Delta V_{mt} = V_{mt_0}$ the initial value, assuming all mechanically trapped gas is removed upon pressurization because of solubility.

4) Residual gas volume $\Delta V_r = V_{r_0}$ the initial value, assuming all gas adhering to cell plates is removed upon pressurization because of solubility.

5) Electrolysis of water volume lost due to gassing overcharge,

$$\Delta V_e = \alpha_e K C N$$

where

α_e = 0.34 cm³/amp-hr
K = gassing overcharge factor
C = cell capacity
N = cycles between battery maintenance

6) Volume change due to cell chemical change, ΔV_{cc}, can vary with cell conditions and contamination. Initially, there is a slight volume reduction upon discharge, but the relatively large loss of electrolyte volume is essentially made up by the production of lead sulphate.

The initial fill volume of the reservoir should be

$$V_{\text{fill}} = \Delta V_c + \alpha_t V_o (T_{\text{fill}} - T_{\min}) + \Delta V_{\text{mt}} + \Delta V_r + \Delta V_e + \Delta V_{cc}$$

which is true if the cell is charged and known to contain residual gas. The oil column above the electrolyte to the acid removal baffles should be at least

$$V_{\text{above}} = \alpha_t V_o (T_{\max} - T_{\text{fill}})$$

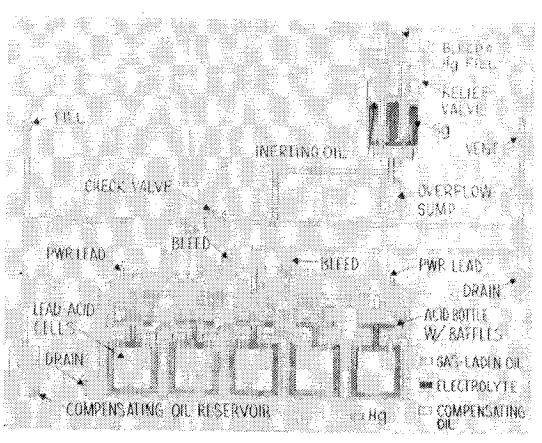

Fig. 2 Industrial cell installation schematic.

This volume should also include ΔV_r if any doubt exists as to the presence of residual gas.

Compensator and Relief Valve

The system pressure compensator should be sized to provide a compensating oil supply for the prescribed dive depth and temperature. It should also provide a reserve capacity to compensate for trapped gas volumes and system or relief valve leakage. The minimum compensation volume should be made up of the following incremental volumes:

1) Reduction of volume of battery box oil due to compression,

$$\Delta V_{op} = (V_{ot}/B_{\text{oil}})\Delta P$$

where

V_{ot} = total oil volume = $V_{ob} + V_{oc} + n\Delta V_e + nV_{\text{above}}$
V_{ob} = volume of oil in battery box
V_{oc} = volume of compensator
n = number of cells
B_{oil} = Bulk modulus of oil
ΔP = dive depth pressure

For ΔV_e and V_{above} see previous discussion.

2) Reduction of battery box oil volume due to temperature change,

$$\Delta V_{ot} = \alpha_{ot}(T_{\text{charge}} - T_{\text{min}})$$

where α_{ot} is volumetric temperature expansion coefficient of oil.

3) Required oil volume to compensate cells,

$$\Delta V_{\text{cells}} = n\,(V_{\text{fill}} = \Delta V_e)$$

For V_{fill} and ΔV_e see previous discussion.

4) Required oil volume to accommodate oil lost through relief valve and through leakage is ΔV_1

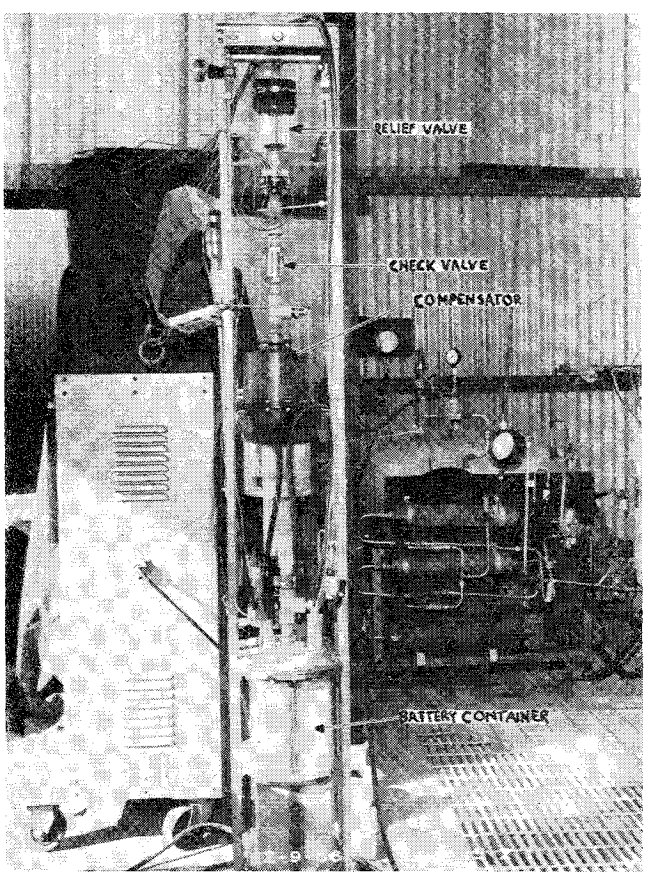

Fig. 3 Industrial cell test assembly.

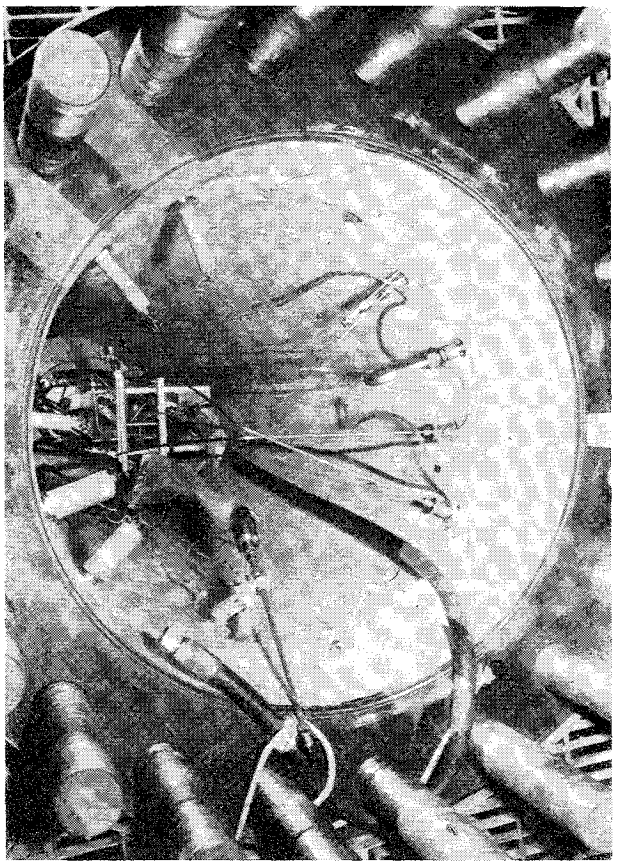

Fig. 4 Pressure test chamber.

5) Required oil volume to compensate mechanically trapped gas $\Delta V_{tg} = V_{tg_0}$ the initial value, assuming that all trapped gas is removed upon pressurization because of solubility.

So, volume of oil compensator should be at least

$$V_{oc} = \Delta V_{op} + \Delta V_{ot} + \Delta V_{\text{cells}} + \Delta V_1 + \Delta V_{tg}$$

The relief valve should be set so that its reseat value is above the maximum compensator pressure so as to minimize the amount of compensating oil carried out with cell gas venting.

Test Program

Figure 2 presents a schematic of a lead-acid battery system meeting the basic requirements mentioned previously with the added provision of an internal manifold system with check valve to prevent gas-contaminated or acid-contaminated oil from contacting the cell terminals. A configuration of this nature was constructed and tested at pressures up to 2700 psi as shown in Figs. 3 and 4. This system contained a single, industrial-type, lead-acid cell of 780 amp-hr rating. A configuration was also tested which contained a 12-v, automotive-type battery of 220-amp-hr rating. The terminals were potted and a differential density head type compensator was used (see Figs. 5 and 6.)

The test program was conducted in three phases as follows: 1) to establish the system's performance level prior to submersion for the pressure testing, 2) the pressurization tests in which the cells were discharged at different rates and various pressures up to 2700 psi (6000-ft dive), and 3) post-submersion tests, in which the effects of phase 2 testing could be evaluated. Throughout the testing, data were obtained on several aspects of cell and system performance, some of which are as follows: capacity at temperature and pressure; charging, schedule, and acceptance; cell gassing during charge, discharge, and standby; management of acid-oil interface level, residual gas

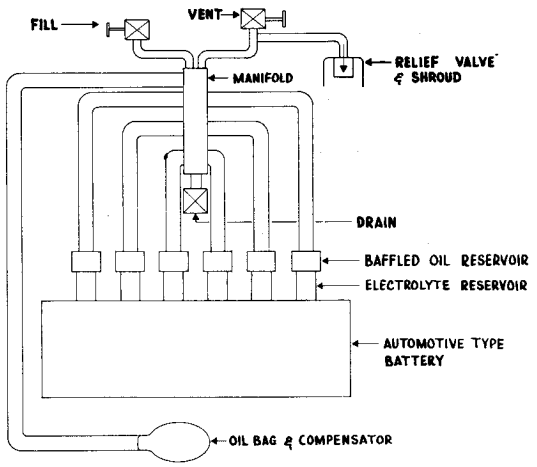

Fig. 5 Automotive battery installation schematic.

retention; and management of compensator oil charge, relief valve performance.

The immediate results of the test program were the verification of considerable performance criteria. The premium here is the fact that results were obtained in a deep-submergence atmosphere with representative hardware. It was then possible to correlate performance deviations, when they occurred, with hardware degradation, when it was observed.

Capacity

Preliminary testing on candidate cells was conducted to demonstrate their ability to arrive at advertised capacity values. In one instance, this was not the case, as several cells of the same type fell short of published values by as much as 21%. It was also possible to observe the initial capacity performance of the heavy-duty, industrial-type, lead-acid cell, as compared to the automotive type. Cold temperature tests were also performed at atmospheric pressure to verify capacity degradation at reduced temperature.

Phase 2 tests, conducted at various pressures up to 2700 psi and at different rates, generated a set of capacity curves at

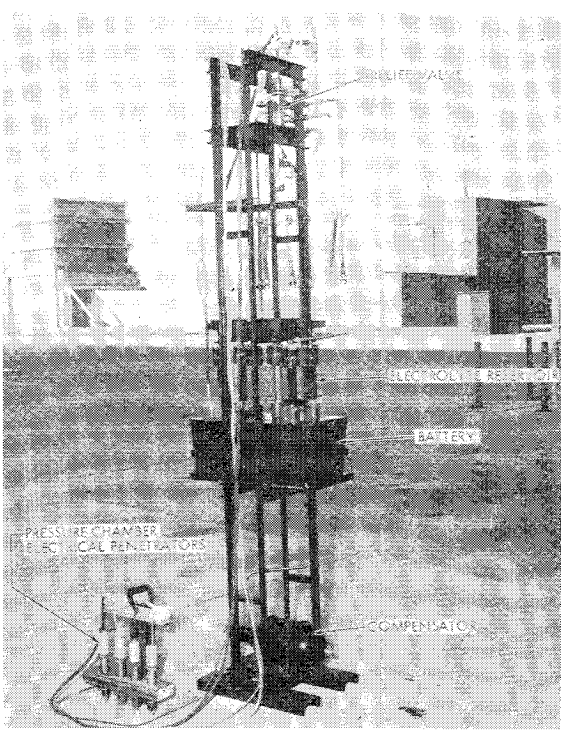

Fig. 6 Automotive battery test assembly.

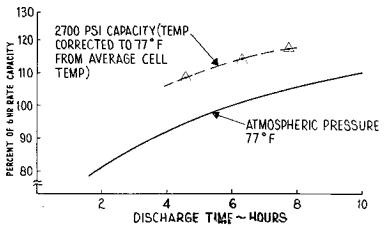

Fig. 7 Pressure effect on capacity.

increased pressures. Figure 7 shows the capacity vs discharge rate at 2700 psi for a 780 amp-hr, industrial-type, lead-acid cell. These data have been temperature-corrected for comparison with a standard capacity curve at 77°F.

After 17 cycles of deep discharge, six of which have been at increased pressures, the industrial cell was still delivering the rated capacity as was anticipated. The 12-v, automotive-type, battery capacity, after 15 cycles of deep discharge, was 12% below anticipated capacity from an initial high of 108%. One cell was acting up and took charge with difficulty in phase 3 testing.

Charging

Throughout a large part of the test program, charge sequence was accomplished to the convenience of the discharge schedules. Charging was normally conducted overnight with one check and reset point. Final charge was verified by voltage leveling off above 2.6 and by overcharge percentage. A charge test was conducted on the industrial cell, in which the measurable parameters of current, voltage, gravity, temperature, and gassing rate were monitored. The charge was manually controlled throughout the sequence. A maximum capacity charge current of 160 amp was maintained for $3\frac{3}{4}$ hr to reach the temperature voltage gassing (TVG) point. TVG point defines the charge voltage at a specific temperature at which cell gassing commences. The charge current was then reduced in increments maintaining the voltage close to the TVG value until the finish rate of 5% capacity, 40 amp, was reached. Figure 8 is a plot of the charge parameters obtained. It should be noted that the plot of test current almost perfectly follows the theoretical curve, except it has been translated in time to account for the fact that initial charge rate was only about 20% of theoretical maximum. The theoretical curve follows the form $I = Ce^{-t}$ where C equals the amp-hours removed. The maximum initial charge current for a 100% discharge would be 780 amp. The accumulated capacity to the finish current value was 737 amp-hr, as compared to 741 for integration under the exponential curve. This close correlation demonstrates that the two methods of charge control are, in fact, the same, and TVG control is defined for chargers with maximum charge current less than the C rate, as well as not being dependent on previous charge history. Cell-gassing increase during charging indicates that the ampere rate is exceeding the acceptance rate. At the end of the finish charge, all of the charge current would be producing gas (approximately 11 cm^3 of H_2 and O_2/amp/min/cell).

Gassing

In addition to cell gassing during charge, gassing was also monitored during discharge and standby. Gassing rate during discharge does not appear to be a steady or repeatable phenomenon, as data varied from cell to cell and from cycle to cycle, primarily in the earlier cycles on each cell. Figure 9 shows a record of cell gassing during a 6-hr discharge cycle. It also depicts cell gassing during standby conditions, in which it reduced to a minimum value several hours after charge termination, where it remained nearly constant. Standby gas was found to be mostly hydrogen. One factor that has a large influence on cell top reservoir and compensator sizing is

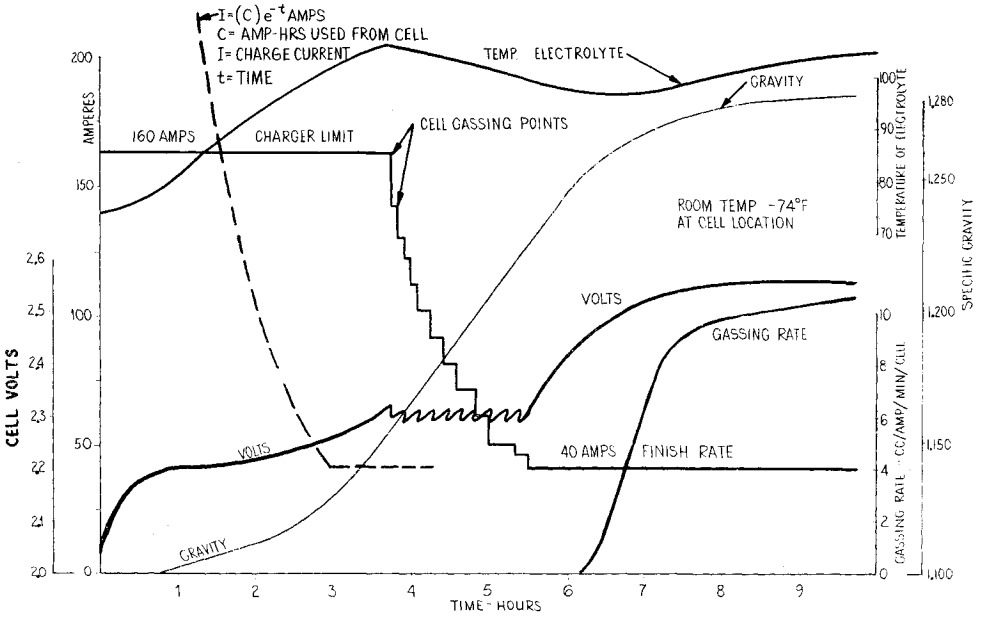

Fig. 8 Charging characteristics.

the residual gas retention of various cell types. Large volumes of gas can remain on plates, raising the electrolyte level. Then vibration shock and application of pressure will reduce this volume, thus lowering the electrolyte level. Results of testing showed the residual gas retention of the industrial-type cell to not exceed manufacturer-stated values of $\frac{1}{2}$ cm³ per amp-hr of cell capacity for this type construction. The gas retention by the pasted plate-type automotive battery, on the other hand, was found to exceed this value so cell top reservoirs and compensator volumes would have to be proportionately larger for this type construction.

Venting

Two types of gas vent valves were utilized in the system test program. One was a poppet-type with a cracking pressure of $1\frac{1}{2}$ psi. To provide a backup design for this conventional type, a heavy fluid trap valve was constructed and installed in the industrial cell ICR system. The problems that could be encountered with conventional vent valves are sticking when operated in a fouling atmosphere with the result that seawater enters the battery box or compensating oil is lost if even a small leak is maintained over a period of time. The advantages of a fluid trap valve are that it is leak-proof, jam-proof, and maintains an accurate cracking pressure. The conventional poppet-type valve permitted loss of compensating oil during phase 2 system tests, because of contamination of its poppet seat. Although the fluid trap vent valve did not suffer this problem, it will have to be maintained periodically to ensure that the fluid does not oxidize excessively in the seawater environment. It is possible to place a thin film of inert, high-density oil over the trap fluid to impede any chemical action that may occur.

During the phase 2 testing of the industrial cell, an intentional malfunction test was performed. The purpose of this test was to simulate excessive gassing and test the elimination of same by the venting system. The gassing was produced by additionally charging the fully charged cell at a 100-amp rate for $\frac{1}{2}$ hr, while the cell and its ICR system were submerged and pressurized to 2700 psi. As the system was depressurized, no malfunctions were encountered and 42,000 cm³ of gas were successfully expelled by the venting system.

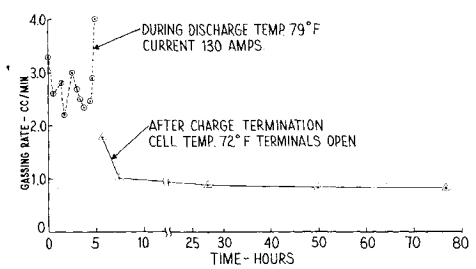

Fig. 9 Gassing characteristics of 780 amp-hr, lead-acid cell.

Conclusion

The results of this test program are encouraging in that the performance of the industrial cell capacity was commendable and that it showed good repeatability throughout the testing. The performance of the cell's insulation compensation and gas-removal system was essentially as anticipated. It is felt that this system concept, with minor modifications, is suitable for establishment of guidelines for the battery power system for the North American Beaver Mark IV design now in progress.

References

[1] Solomon, F. and Work, G. W., "Present-Day Long Life Silver-Zinc Secondary Batteries," *Proceedings of the 4th International Symposium on Research and Development in Nonmechanical Electrical Power Sources, Brighton, England,* Sept. 1964.

[2] Keralla, J. A. and Lander, J. J., "Sealed Zinc-Silver Oxide Batteries," *16th Annual Power Sources Conference,* May 1962.